

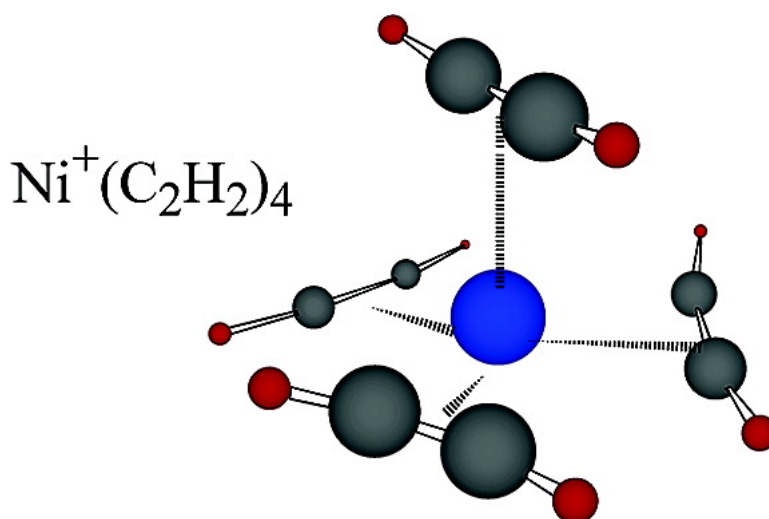
Article

Vibrational Spectroscopy and Structures of Ni(CH) ($n=1-4$) Complexes

Richard S. Walters, E. Dinesh Pillai, Paul v. R. Schleyer, and Michael A. Duncan

J. Am. Chem. Soc., **2005**, 127 (48), 17030-17042 • DOI: 10.1021/ja054800r • Publication Date (Web): 03 November 2005

Downloaded from <http://pubs.acs.org> on March 25, 2009



More About This Article

Additional resources and features associated with this article are available within the HTML version:

- Supporting Information
- Links to the 4 articles that cite this article, as of the time of this article download
- Access to high resolution figures
- Links to articles and content related to this article
- Copyright permission to reproduce figures and/or text from this article

[View the Full Text HTML](#)



ACS Publications
High quality. High impact.

Vibrational Spectroscopy and Structures of Ni⁺(C₂H₂)_n (n = 1–4) Complexes

Richard S. Walters, E. Dinesh Pillai, Paul v. R. Schleyer, and Michael A. Duncan*

Contribution from the Department of Chemistry, University of Georgia, Athens, Georgia 30602-2556

Received July 18, 2005; E-mail: maduncan@uga.edu

Abstract: Nickel cation–acetylene complexes of the form Ni⁺(C₂H₂)_n, Ni⁺(C₂H₂)Ne, and Ni⁺(C₂H₂)_nAr_m (n = 1–4) are produced in a molecular beam by pulsed laser vaporization. These ions are size-selected and studied in a time-of-flight mass spectrometer by infrared laser photodissociation spectroscopy in the C–H stretch region. The fragmentation patterns indicate that the coordination number is 4 for this system. The n = 1–4 complexes with and without rare gas atoms are also investigated with density functional theory. The combined IR spectra and theory show that π-complexes are formed for the n = 1–4 species, causing the C–H stretches in the acetylene ligands to shift to lower frequencies. Theory reveals that there are low-lying excited states nearly degenerate with the ground state for all the Ni⁺(C₂H₂)_n complexes. Although isomeric structures are identified for rare gas atom binding at different sites, the attachment of rare gas atoms results in only minor perturbations on the structures and spectra for all complexes. Experiment and theory agree that multiple acetylene binding takes place to form low-symmetry structures, presumably due to Jahn–Teller distortion and/or ligand steric effects. The fully coordinated Ni⁺(C₂H₂)₄ complex has a near-tetrahedral structure.

Introduction

Transition metal–olefin complexes play an important role in catalysis and have been studied extensively in organometallic chemistry.^{1,2} Gas-phase organometallic ion complexes are convenient models to study π-bonding, and these systems have been probed experimentally using mass spectrometry.^{3–13} Reactions of transition metals with hydrocarbons and the details of

their binding energetics have been studied in gas-phase ion chemistry,^{3–13} and many of these systems have been investigated with theory.^{14–21} Electronic spectroscopy has been applied to

- (1) Heck, R. F. *Organotransition Metal Chemistry*; Academic Press: New York, 1974.
(2) Jolly, P. W.; Wilke, G. *The Organic Chemistry of Nickel*; John Wiley: New York, 1974.
(3) (a) Eller, K.; Schwarz, H. *Chem. Rev.* **1991**, *91*, 1121. (b) Wesendrup, R.; Schwarz, H. *Organometallics* **1997**, *16*, 461. (c) Schroeder, K.; Schalley, C. A.; Wesendrup, R.; Schroeder, D.; Schwarz, H. *Organometallics* **1997**, *16*, 986. (d) Harvey, J. N.; Diefenbach, M.; Schroeder, D.; Schwarz, H. *Int. J. Mass Spectrom.* **1999**, *182*, 85. (e) Schwarz, H. *Angew. Chem., Int. Ed.* **2003**, *42*, 4442. (f) Bohme, D. K.; Schwarz, H. *Angew. Chem., Int. Ed.* **2005**, *44*, 2336.
(4) Tonkyn, R.; Ronan, M.; Weisshaar, J. C. *J. Phys. Chem.* **1988**, *92*, 92.
(5) (a) Zemski, K. A.; Bell, R. C.; Castleman, A. W., Jr. *J. Phys. Chem. A* **2000**, *104*, 5732. (b) Zemski, K. A.; Justes, D. R.; Castleman, A. W., Jr. *J. Phys. Chem. A* **2001**, *105*, 10237. (c) Justes, D. R.; Mitrić, R.; Moore, N. A.; Bonačić-Koutecký, V.; Castleman, A. W., Jr. *J. Am. Chem. Soc.* **2003**, *125*, 6289.
(6) (a) Armentrout, P. B.; Beauchamp, J. L. *J. Am. Chem. Soc.* **1981**, *103*, 784. (b) Elkind, J. L.; Armentrout, P. B. *J. Am. Chem. Soc.* **1986**, *108*, 2765. (c) Aristov, N.; Armentrout, P. B. *J. Am. Chem. Soc.* **1986**, *108*, 1806. (d) Georgiadis, R.; Armentrout, P. B. *Int. J. Mass Spectrom. Ion Processes* **1989**, *89*, 227. (e) Fisher, E. R.; Armentrout, P. B. *J. Phys. Chem.* **1990**, *94*, 1674. (f) Meyer, F.; Khan, F. A.; Armentrout, P. B. *J. Am. Chem. Soc.* **1995**, *117*, 9740. (g) Sievers, M. R.; Jarvis, L. M.; Armentrout, P. B. *J. Am. Chem. Soc.* **1998**, *120*, 1891. (h) Sievers, M. R.; Chen, Y.-M.; Haynes, C. L.; Armentrout, P. B. *Int. J. Mass Spectrom.* **2000**, *195*, 149. (i) van Koppen, P. A. M.; Bowers, M. T.; Haynes, C. L.; Armentrout, P. B. *J. Am. Chem. Soc.* **1998**, *120*, 5704. (j) Rodgers, M. T.; Armentrout, P. B. *Mass Spectrom. Rev.* **2000**, *19*, 215. (k) Armentrout, P. B. *Annu. Rev. Phys. Chem.* **2001**, *52*, 423. (l) Tjelte, B. L.; Walter, D.; Armentrout, P. B. *Int. J. Mass Spectrom.* **2001**, *204*, 7. (m) Armentrout, P. B. *Int. J. Mass Spectrom.* **2003**, *227*, 289. (n) Armentrout, P. B. *Eur. J. Mass Spectrom.* **2003**, *9*, 531. (o) Rogers, M. T.; Armentrout, P. B. *Compr. Coord. Chem.* **2004**, *2*, 141.
(7) (a) van Koppen, P. A. M.; Kemper, P. R.; Bushnell, J. E.; Bowers, M. T. *J. Am. Chem. Soc.* **1995**, *117*, 2098. (b) Gidden, J.; van Koppen, P. A. M.; Bowers, M. T. *J. Am. Chem. Soc.* **1997**, *119*, 3935. (c) Kemper, P. R.; Bushnell, J.; Bowers, M. T.; Gellene, G. I. *J. Phys. Chem. A* **1998**, *102*, 8590. (d) van Koppen, P. A. M.; Perry, J. K.; Kemper, P. R.; Bushnell, J. E.; Bowers, M. T. *Int. J. Mass Spectrom.* **1999**, *185*, 989. (e) Manard, M. J.; Kemper, P. R.; Carpenter, C. J.; Bowers, M. T. *Int. J. Mass Spectrom.* **2005**, *241*, 99. (f) Manard, M. J.; Kemper, P. R.; Bowers, M. T. *Int. J. Mass Spectrom.* **2005**, *241*, 109.
(8) Gibson, J. K. *J. Organomet. Chem.* **1998**, *558*, 51.
(9) Hanmura, T.; Ichihashi, M.; Kondow, T. *J. Phys. Chem. A* **2002**, *106*, 11465.
(10) Beyer, M. K.; Berg, C. B.; Bondybey, V. E. *Phys. Chem. Chem. Phys.* **2001**, *3*, 1840.
(11) (a) Freiser, B. S., Ed. *Organometallic Ion Chemistry*; Kluwer: Dordrecht, The Netherlands, 1996. (b) Ranatunga, D. R. A.; Freiser, B. S. *Chem. Phys. Lett.* **1995**, *233*, 319. (c) Surya, P. I.; Roth, L. M.; Ranatunga, D. R. A.; Freiser, B. S. *J. Am. Chem. Soc.* **1996**, *118*, 1118. (d) Chen, Q.; Auberry, K. J.; Freiser, B. S. *Int. J. Mass Spectrom. Ion Processes* **1998**, *175*, 1.
(12) Dunbar, R. C. *Int. J. Mass Spectrom.* **2000**, *200*, 571.
(13) (a) Willey, K. F.; Cheng, P. Y.; Bishop, M. B.; Duncan, M. A. *J. Am. Chem. Soc.* **1991**, *113*, 4721. (b) Willey, K. F.; Yeh, C. S.; Robbins, D. L.; Duncan, M. A. *J. Phys. Chem.* **1992**, *96*, 9606. (c) Reddic, J. E.; Robinson, J. C.; Duncan, M. A. *Chem. Phys. Lett.* **1997**, *279*, 203. (d) Buchanan, J. W.; Reddic, J. E.; Grieves, G. A.; Duncan, M. A. *J. Phys. Chem. A* **1998**, *102*, 6390. (e) Buchanan, J. W.; Grieves, G. A.; Reddic, J. E.; Duncan, M. A. *Int. J. Mass Spectrom.* **1999**, *182*, 323. (f) Foster, N. R.; Grieves, G. A.; Buchanan, J. W.; Flynn, N. D.; Duncan, M. A. *J. Phys. Chem. A* **2000**, *104*, 11055.
(14) (a) Sodupe, M.; Bauschlicher, C. W., Jr. *J. Phys. Chem.* **1991**, *95*, 8640. (b) Sodupe, M.; Bauschlicher, C. W., Jr.; Langhoff, S. R.; Partridge, H. *J. Phys. Chem.* **1992**, *96*, 2118.
(15) (a) Hertwig, R. H.; Koch, W.; Schroeder, D.; Schwarz, H.; Hrusak, J.; Schwerdtfeger, P. *J. Phys. Chem.* **1996**, *100*, 12253. (b) Holthausen, M. C.; Fiedler, A.; Schwarz, H.; Koch, W. *J. Phys. Chem.* **1996**, *100*, 6236. (c) Stoekigt, D.; Schwarz, J.; Schwarz, H. *J. Phys. Chem.* **1996**, *100*, 8786. (16) (a) Frenking, G.; Fröhlich, N. *Chem. Rev.* **2000**, *100*, 717. (b) Nechaev, M. S.; Rayon, V. M.; Frenking, G. *J. Phys. Chem. A* **2004**, *108*, 3134. (17) Klippenstein, S. J.; Yang, C.-N. *Int. J. Mass Spectrom.* **2000**, *201*, 253. (18) Pandey, R.; Rao, B. K.; Jena, P.; Alvarez-Blanco, M. *J. Am. Chem. Soc.* **2001**, *123*, 3799.

some metal ion π -complexes with acetylene or ethylene,^{22–24} but only limited data is available on these systems in their ground states. Infrared and Raman spectroscopies are often applied to organometallic compounds in the condensed phase,^{25–31} but these methods are problematic for ions in the gas phase because of the low sample densities. However, recent advances in technology now make it possible to study gas-phase metal ion complexes by infrared laser photodissociation (IRPD) spectroscopy.^{32–44} In this paper, we report IRPD spectroscopy

for Ni⁺(C₂H₂)_n complexes ($n = 1–4$). Vibrational spectra in the C–H stretch region are compared to harmonic frequencies calculated with density functional theory (DFT), allowing determination of the structures and bonding patterns in these systems.

Metal ion complexes have been studied for many years with a variety of techniques in mass spectrometry. Several groups have studied reactions of transition metal ions with different hydrocarbons.^{3–10} Photodissociation has been employed to observe fragmentation pathways and to determine the binding energies of metal ion π -complexes.^{11–13} Bond energies have also been determined with equilibrium mass spectrometry^{7,8,12} and collision-induced dissociation.^{6–8} The geometric and electronic structures of metal ion π -complexes have been investigated with theory by a number of groups.^{14–21} This work has focused on the interplay between electrostatic and covalent forces that are involved in the metal–olefin π bond. Bauschlicher used the modified coupled pair functional (MCPF) methodology.¹⁴ Schwarz and co-workers determined that π -back-bonding was as important as σ -donation for M⁺–ethylene (M = Cu, Ag, Au) using DFT and Hartree–Fock/DFT hybrid methods.¹⁵ More recently, Frenking has incorporated an energy partitioning analysis into DFT and ab initio computations to describe which forces dominate in a variety of organometallic complexes.¹⁶ Of particular interest to this paper, Klippenstein studied various metal ion π -complexes, including Ni⁺–acetylene, with DFT and reported on fundamental vibrational shifts caused by π -bonding.¹⁷

Spectroscopic studies of metal ion complexes have been difficult because of the low sample densities and because ions are often produced at high temperature from conventional sources, leading to extensive fragmentation. However, new molecular beam sources make it possible to produce cation–molecular adducts without fragmentation, enabling spectroscopic studies. Our group²² and that of Klieber²³ have studied Mg⁺ and Ca⁺ π -complexes with acetylene and ethylene by electronic photodissociation spectroscopy, revealing detailed information on their excited states. Recently, Metz and co-workers have used similar techniques to study Pt⁺(C₂H₄) and Au⁺(C₂H₄).²⁴ However, all these studies were limited to single ligand complexes with metal ions that have transitions accessible with tunable dye lasers. Many transition metal complexes are difficult to study with electronic spectroscopy because they have no convenient absorption. Especially for those complexes with multiple ligands, predissociation in excited electronic states is efficient, often producing structureless spectra.

- (19) Chaquin, P.; Costa, D.; Lepetit, C.; Che, M. *J. Phys. Chem. A* **2001**, *105*, 4541.
- (20) Sicilia, E.; Russo, N. *J. Mol. Struct.* **2004**, *709*, 167.
- (21) Straub, B. F.; Gollub, C. *Chem. Eur. J.* **2004**, *10*, 3081.
- (22) (a) Duncan, M. A. *Annu. Rev. Phys. Chem.* **1997**, *48*, 63. (b) France, M. R.; Pullins, S. H.; Duncan, M. A. *J. Chem. Phys.* **1998**, *109*, 8842. (c) Reddic, J. E.; Duncan, M. A. *Chem. Phys. Lett.* **1999**, *312*, 96. (d) Weslowski, S. S.; King, R. A.; Schaefer, H. F.; Duncan, M. A. *J. Chem. Phys.* **2000**, *113*, 701.
- (23) (a) Chen, J.; Wong, T. H.; Cheng, Y. C.; Montgomery, K.; Kleiber, P. D. *J. Chem. Phys.* **1998**, *108*, 2285. (b) Chen, J.; Wong, T. H.; Kleiber, P. D.; Wang, K. H. *J. Chem. Phys.* **1999**, *110*, 11798. (c) Kleiber, P. D. *Adv. Metal Semicond. Clusters* **2001**, *5*, 267. (d) Lu, W.-Y.; Liu, R.-G.; Wong, T.-H.; Chen, J.; Kleiber, P. D. *J. Phys. Chem. A* **2002**, *106*, 725.
- (24) (a) Metz, R. B. *Int. Rev. Chem.* **2004**, *23*, 79. (b) Aguirre, F.; Husband, J.; Thompson, C. J.; Metz, R. B. *Chem. Phys. Lett.* **2000**, *318*, 466. (c) Husband, J.; Aguirre, F.; Thompson, C. J.; Laperle, C. M.; Metz, R. B. *J. Phys. Chem. A* **2000**, *104*, 2020. (d) Stringer, K. L.; Citir, M.; Metz, R. B. *J. Phys. Chem. A* **2004**, *108*, 6996.
- (25) Nakamoto, K. *Infrared and Raman Spectra of Inorganic and Coordinated Compounds*, 5th ed.; John Wiley: New York, 1997; Vols. A, B.
- (26) (a) Chatt, J.; Rowe, G. A.; Williams, A. A. *Proc. Chem. Soc.* **1957**, 208. (b) Chatt, J.; Duncanson, L. A.; Guy, R. G. *J. Chem. Soc.* **1961**, 827. (c) Chatt, J.; Duncanson, L. A.; Guy, R. G.; Thompson, D. T. *J. Chem. Soc.* **1963**, 5170.
- (27) Greaves, E. O.; Lock, C. J. L.; Maitlis, P. M. *Can. J. Chem.* **1968**, *46*, 3879.
- (28) (a) Dosa, P. I.; Whitener, G. D.; Vollhardt, K. P. C.; Bond, A. D.; Teat, S. J. *Org. Lett.* **2002**, *4*, 2075. (b) Diercks, R.; Eaton, B. E.; Guertzen, S.; Jalisatgi, S.; Matzger, A. J.; Radde, R. H.; Vollhardt, K. P. C. *J. Am. Chem. Soc.* **1998**, *120*, 8247. (c) Colborn, R. E.; Vollhardt, K. P. C. *J. Am. Chem. Soc.* **1986**, *108*, 5470. (d) Colborn, R. E.; Vollhardt, K. P. C. *J. Am. Chem. Soc.* **1981**, *103*, 6259.
- (29) Ozin, G. A.; McIntosh, D. F.; Power, W. J.; Messmer, R. P. *Inorg. Chem.* **1981**, *20*, 1782.
- (30) Kline, E. S.; Kafafi, Z. H.; Hauge, R. H.; Margrave, J. L. *J. Am. Chem. Soc.* **1987**, *109*, 2402.
- (31) (a) Manceron, L.; Andrews, L. *J. Phys. Chem.* **1989**, *93*, 2964. (b) Burkholder, T. R.; Andrews, L. *Inorg. Chem.* **1993**, *32*, 2491. (c) Thompson, C. A.; Andrews, L. *J. Am. Chem. Soc.* **1996**, *118*, 10242.
- (32) (a) Weinheimer, C. J.; Lisy, J. M. *J. Chem. Phys.* **1996**, *105*, 2938. (b) Lisy, J. M. *Int. Rev. Phys. Chem.* **1997**, *16*, 267. (c) Cabarcos, O. M.; Weinheimer, C. J.; Lisy, J. M. *J. Chem. Phys.* **1998**, *108*, 5151. (d) Cabarcos, O. M.; Weinheimer, C. J.; Lisy, J. M. *J. Chem. Phys.* **1999**, *110*, 8429. (e) Vaden, T. D.; Forinash, B.; Lisy, J. M. *J. Chem. Phys.* **2002**, *117*, 4628. (f) Patwari, G. N.; Lisy, J. M. *J. Chem. Phys.* **2003**, *118*, 8555. (g) Vaden, T. D.; Weinheimer, C. J.; Lisy, J. M. *J. Chem. Phys.* **2004**, *121*, 3102.
- (33) (a) Gregoire, G.; Velasquez, J.; Duncan, M. A. *Chem. Phys. Lett.* **2001**, *349*, 451. (b) Gregoire, G.; Duncan, M. A. *J. Chem. Phys.* **2002**, *117*, 2120.
- (34) (a) Gregoire, G.; Brinkman, N. R.; Schaefer, H. F.; Duncan, M. A. *J. Phys. Chem. A* **2003**, *107*, 218. (b) Walters, R. S.; Jaeger, T. D.; Brinkman, N. R.; Schaefer, H. F.; Duncan, M. A. *J. Phys. Chem. A* **2003**, *107*, 7396. (c) Jaeger, J. B.; Jaeger, T. D.; Brinkman, N. R.; Schaefer, H. F.; Duncan, M. A. *Can. J. Chem.* **2004**, *82*, 934.
- (35) Duncan, M. A. *Int. Rev. Phys. Chem.* **2003**, *22*, 407.
- (36) (a) Walker, N. R.; Grieves, G. A.; Walters, R. S.; Duncan, M. A. *Chem. Phys. Lett.* **2003**, *380*, 230. (b) Walker, N. R.; Walters, R. S.; Duncan, M. A. *J. Chem. Phys.* **2004**, *120*, 10037. (c) Walker, N. R.; Grieves, G. A.; Walters, R. S.; Duncan, M. A. *J. Chem. Phys.* **2004**, *121*, 10498.
- (37) (a) Walters, R. S.; Jaeger, T. D.; Duncan, M. A. *J. Phys. Chem. A* **2002**, *106*, 10482. (b) Walters, R. S.; Schleyer, P. v. R.; Corminboeuf, C.; Duncan, M. A. *J. Am. Chem. Soc.* **2005**, *127*, 1100.
- (38) (a) Jaeger, T. D.; Pillai, E. D.; Duncan, M. A. *J. Phys. Chem. A* **2004**, *108*, 6605. (b) Jaeger, T. D.; Duncan, M. A. *J. Phys. Chem. A* **2005**, *109*, 3311.
- (39) (a) Walker, N. R.; Walters, R. S.; Pillai, E. D.; Duncan, M. A. *J. Chem. Phys.* **2003**, *119*, 10471. (b) Walters, R. S.; Duncan, M. A. *Austr. J. Chem.* **2004**, *57*, 1145. (c) Walker, N. R.; Walters, R. S.; Jordan, K. D.; Duncan, M. A. *J. Phys. Chem. A* **2005**, *109*, 7057.
- (40) Pillai, E. D.; Jaeger, T. D.; Duncan, M. A. *J. Phys. Chem. A* **2005**, *109*, 3521.
- (41) (a) van Heijnsbergen, D.; von Helden, G.; Meijer, G.; Maitre, P.; Duncan, M. A. *J. Am. Chem. Soc.* **2002**, *124*, 1562. (b) van Heijnsbergen, D.; Jaeger, T. D.; von Helden, G.; Meijer, G.; Duncan, M. A. *Chem. Phys. Lett.* **2002**, *364*, 345. (c) Jaeger, T. D.; van Heijnsbergen, D.; Klippenstein, S. J.; von Helden, G.; Meijer, G.; Duncan, M. A. *J. Am. Chem. Soc.* **2004**, *126*, 10981.
- (42) (a) Simon, A.; Jones, W.; Ortega, J.-M.; Boissel, P.; Lemaire, J.; Maitre, P. *J. Am. Chem. Soc.* **2004**, *126*, 11666. (b) Le Caer, S.; Heninger, M.; Maitre, P.; Mestdagh, H. *Rapid Commun. Mass Spectrom.* **2003**, *17*, 351. (c) Lemaire, J.; Boissel, P.; Heninger, M.; Mauclair, G.; Bellec, G.; Mestdagh, H.; Simon, A.; Le Caer, S.; Ortega, J. M.; Glotin, F.; Maitre, P. *Phys. Rev. Lett.* **2002**, *89*, 273002. (d) Le Caer, S.; Heninger, M.; Lemaire, J.; Boissel, P.; Maitre, P.; Mestdagh, H. *Chem. Phys. Lett.* **2000**, *385*, 273. (e) Reinhard, B. M.; Lagutschenkov, A.; Lemaire, J.; Maitre, P.; Boissel, P.; Niedner-Schatteburg, G. *J. Phys. Chem. A* **2004**, *108*, 3350.
- (43) (a) Oomens, J.; Moore, D. T.; von Helden, G.; Meijer, G.; Dunbar, R. C. *J. Am. Chem. Soc.* **2004**, *126*, 724. (b) Moore, D. T.; Oomens, J.; Eyler, J. R.; Meijer, G.; von Helden, G.; Ridge, D. P. *J. Am. Chem. Soc.* **2004**, *126*, 14726. (c) Fielicke, A.; von Helden, G.; Meijer, G.; Petersen, D. B.; Simard, B.; Rayner, D. M. *J. Phys. Chem. B* **2004**, *108*, 14591. (d) Moore, D. T.; Oomens, J.; Eyler, J. R.; von Helden, G.; Meijer, G.; Dunbar, R. C. *J. Am. Chem. Soc.* **2005**, *127*, 7243. (e) Fielicke, A.; von Helden, G.; Meijer, G.; Pederson, D. B.; Simard, B.; Rayner, D. M. *J. Am. Chem. Soc.* **2005**, *127*, 8416.
- (44) (a) Inokuchi, Y.; Ohshimo, K.; Misaizu, F.; Nishi, N. *J. Phys. Chem. A* **2004**, *108*, 5034. (b) Inokuchi, Y.; Ohshimo, K.; Misaizu, F.; Nishi, N. *Chem. Phys. Lett.* **2004**, *390*, 140.

Infrared spectroscopy has been a mainstay in organometallic chemistry since the first metal–acetylene complexes were reported.^{25–27} For example, Maitlis and co-workers studied nickel–acetylene complexes by IR spectroscopy in the C≡C stretch region.²⁷ From these and similar studies on metal–ethylene and metal–carbonyl complexes,^{1,25–28} a qualitative picture of the metal–molecular interaction known as the Dewar–Chatt–Duncanson (DCD) π -bonding model was developed. In all these systems, there are different degrees of σ -type donation from the filled π bonding orbitals of acetylene into the empty metal orbitals, and π -type back-donation from the filled metal d orbitals into the π^* antibonding of acetylene. Both factors weaken the bonding in acetylene, lowering its vibrational frequencies. Most condensed-phase metal–acetylene studies have focused on how the π -interaction affects the C≡C stretch in the olefin subunit, as this mode is commonly the most perturbed.^{25–28} However, condensed-phase IR spectra are often congested due to overlapping vibrational transitions and solvent effects. For unstable systems, IR spectroscopy of metal–olefins has also been investigated using rare gas matrix isolation.^{29–31}

It is clear that IR spectroscopy would also be desirable to investigate gas-phase ion systems. However, until recently, such experiments were not possible. The low density of ions that can be produced precludes absorption spectroscopy, and the intense and tunable infrared lasers needed for techniques such as photodissociation were not available. Fortunately, recent advances in IR laser technology have now been combined with mass spectrometry, making it possible to study a variety of size-selected cation–molecular complexes.^{32–44} IRPD spectroscopy was first reported by the Lisy group³² on alkali cation complexes produced from thermal ion sources and studied with tunable optical parametric oscillator (OPO) lasers. Our group combined similar OPO lasers with pulsed-nozzle laser vaporization sources to study both main group and transition metal cation complexes with a variety of small molecules.^{33–40} In collaboration with the Dutch group of Meijer and co-workers, we also studied cation–benzene complexes with a free electron laser (FEL) in the lower frequency region of the IR (200–1600 cm^{-1}).⁴¹ Other groups have now joined this effort on cation–molecular vibrational spectroscopy using both OPO and FEL lasers.^{42–44} In the first IR work on metal–acetylene systems, we reported a study of $\text{Ni}^+(\text{C}_2\text{H}_2)_n$ complexes ($n = 3–6$) with IRPD spectroscopy in the C–H stretching region.^{37a} This study provided preliminary evidence for cyclization chemistry that took place only when second-sphere ligands were present. In a recent communication, we reported similar IRPD spectroscopy of monoacetylene complexes for different transition metal cations (V, Fe, Co, Ni),^{37b} to investigate the periodic trends in the vibrational patterns. These spectra found red-shifted C–H stretch vibrations, consistent with the general predictions of the DCD framework, that varied systematically with the metal. A comparison with theory showed that $\text{Fe}^+(\text{C}_2\text{H}_2)$, $\text{Co}^+(\text{C}_2\text{H}_2)$, and $\text{Ni}^+(\text{C}_2\text{H}_2)$ form π -complexes, while $\text{V}^+(\text{C}_2\text{H}_2)$ forms a three-membered-ring metallacycle. In the present study, we report IRPD spectroscopy and DFT theory for small $\text{Ni}^+(\text{C}_2\text{H}_2)_n$ complexes ($n = 1–4$). Spectroscopy and theory provide detailed information on the ground-state electronic structures and geometries for these systems and how they vary as multiple ligands assemble around the metal cation.

Experimental Section

Nickel ion–acetylene complexes are produced in a pulsed-nozzle laser vaporization source and analyzed with a reflectron time-of-flight mass spectrometer. The source and molecular beam apparatus have been described previously.^{22,33–40} The third harmonic of a Nd:YAG laser (355 nm) is employed to vaporize a rotating nickel rod. $\text{Ni}^+(\text{C}_2\text{H}_2)_n$ clusters are produced in an expansion gas mixture of 5% acetylene in argon. The mixed complexes with rare gas atoms, $\text{Ni}^+(\text{C}_2\text{H}_2)_n\text{Ar}_m$ and $\text{Ni}^+(\text{C}_2\text{H}_2)\text{Ne}$, are produced in expansions containing <1% acetylene in argon or helium:neon, respectively. The pulsed nozzle is from General Valve (Series 9, 1 mm), operating at 50 psi backing pressure with pulse durations near 250 μs . The ions are skimmed into the differentially pumped reflectron time-of-flight mass spectrometer, where they are injected into the first drift region by pulsed acceleration voltages. They are then size-selected by pulsed deflection plates before entering the reflectron field. Photodissociation is accomplished with an IR optical parametric oscillator/amplifier (OPO/OPA) laser at the turning point in the reflectron field. Parent and daughter ions are reaccelerated down the second flight tube and detected using an electron multiplier tube. Data are transferred to a PC by an IEEE interface. Fragmentation is more efficient on resonance; thus, monitoring the fragment ion yield as a function of IR laser wavelength produces the IRPD spectrum of the parent ion that has been mass-selected.

The OPO (LaserVision) uses two KTP crystals pumped by the second harmonic (532 nm) of a Nd:YAG laser (Continuum 9010) to produce tunable 725–872 nm light, which is then combined with the delayed fundamental (1064 nm) in the OPA. The OPA uses four KTA crystals for difference frequency mixing the far-red with the IR fundamental beam, which generates the tunable IR output (2050–4400 cm^{-1}). This tunable IR is then used for IRPD spectroscopy by exciting the ion–molecule complexes near the asymmetric and symmetric C–H stretches of free acetylene (3289 and 3374 cm^{-1}).⁴⁵ The IR frequency is calibrated with the photoacoustic spectrum of methane (2800–3200 cm^{-1}). It should be noted that we did not use this calibration method in our previous work on $\text{Ni}^+(\text{C}_2\text{H}_2)_n$ ($n = 3–6$) complexes.^{37a} The absolute frequencies in the previous work are therefore incorrect by $\sim 14 \text{ cm}^{-1}$, although the relative frequencies are unaffected.

DFT calculations were carried out using the Gaussian03 package (Windows version)⁴⁶ at the B3LYP level of theory.⁴⁷ The 6-31G* and 6-311+G** basis sets were utilized, and we allowed for symmetry breaking to occur during structural optimizations. Vibrational frequencies are scaled by a factor of 0.96, and dissociation energies were not corrected for zero-point energies.

Results and Discussion

Fragmentation Patterns. The mass spectrum of $\text{Ni}^+(\text{C}_2\text{H}_2)_n$ complexes produced in this experiment is similar to that which we reported previously.³⁷ It shows that these complexes grow by simple addition of acetylene molecules around nickel cations without any significant ligand fragmentation. Likewise, in mixed expansions, the masses present are those with intact acetylene and rare gas atoms both bound to the cations. These complexes are size-selected and excited with the IR laser in the C–H stretch region of acetylene (3000–3400 cm^{-1}) to attempt photodissociation. As reported in our previous letter,^{37a} essentially no photodissociation can be detected for the $n = 1–3$ complexes. Beginning with the $n = 4$ complex, the fragmentation yield increases and dissociation occurs by the loss of intact acetylene

(45) Shimanouchi, T. *Molecular Vibrational Frequencies*, 69th ed.; Chemistry WebBook, NIST Standard Reference Database (<http://webbook.nist.gov>), 2001.

(46) Frisch, M. J.; et al. *Gaussian 03*, Revision B.02; Gaussian, Inc.: Pittsburgh, PA, 2003.

(47) (a) Becke, A. D. *J. Chem. Phys.* **1993**, *98*, 5648. (b) Lee, C.; Yang, W.; Parr, R. G. *Phys. Rev. B* **1988**, *37*, 785.

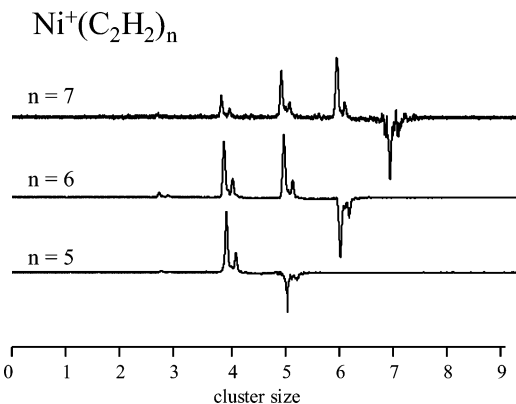


Figure 1. IR photodissociation mass spectra of Ni⁺(C₂H₂)_{5–7}. The negative peaks are the mass-selected parent ions, and the positive peaks are the daughter ions produced by photodissociation. Fragmentation terminates at $n = 4$, suggesting that Ni⁺ prefers a coordination of 4 for this system.

molecules. Resonances are detected near 3100–3300 cm^{−1} for all larger complexes produced (up to about $n = 10$).

The smaller complexes ($n \leq 4$) are hard to dissociate because absorption of IR photons does not provide enough energy to break the metal–ligand bonds. The binding energy of the Ni⁺–C₂H₂ complex has not been measured, but theory predicts it to be about 35.1 kcal/mol,^{14,17,20} which corresponds to ~ 12 300 cm^{−1}. A multiphoton process would therefore be necessary to dissociate this complex near 3200 cm^{−1}. However, multiphoton absorption is inefficient at the laser pulse energies available from our OPO systems. The $n = 2–4$ complexes presumably have all ligands attached directly to the metal. Their bond energies are likely to decrease as binding is distributed to multiple acetylenes, but the per-molecule binding energy may still be greater than 3200 cm^{−1}. As more acetylenes bind to the cluster, the coordination sites around the cation will eventually be filled and additional ligands must attach outside the “core” ligands. Molecules in the second sphere act essentially as solvent and are bound only by van der Waals forces. These should have binding energies similar to that in the acetylene dimer (~ 400 cm^{−1}).^{48,49} Absorption of a single photon could dissociate the larger complexes by eliminating one or more of these weakly bound, second-sphere ligands. The lack of photodissociation signal observed for the smaller complexes and the increase in fragmentation yield for the larger sizes are therefore consistent with the energetics expected for this system.

Figure 1 shows the fragmentation mass spectra of the $n = 5–7$ complexes. The multiplet observed at each cluster size is due to the naturally occurring isotopes of nickel. Data are recorded with the IR laser on and off, and then subtracted from one another to generate these difference spectra. The negative peaks correspond to depletion of the mass-selected parent ion, and the positive peaks are the fragment ions produced by photodissociation. As shown, one or more intact acetylene molecules is eliminated from each parent complex. However, the sequence of elimination steps for all the larger Ni⁺(C₂H₂)_n complexes has a common termination point at the cluster size of $n = 4$. As we have reported for other ion–molecule complexes,³⁶ this termination point in the fragmentation provides

evidence for the stable coordination number for ligand binding around the central metal cation. Weakly bound external ligands are eliminated easily, and the core ion with its strongly bound ligands survives. In this case, Ni⁺ prefers a coordination of four acetylene molecules. We also found a similar coordination number of 4 in our study of Ni⁺(CO₂)_n clusters.^{36a,c} Additionally, Ni(I) prefers to be four-coordinate in either tetrahedral or square-planar configurations in traditional inorganic chemistry.^{50,51}

To acquire the spectra of the small, more strongly bound complexes, we employ a technique known as “rare gas tagging” to improve the fragmentation efficiency. Lee and co-workers were the first to enhance IR photodissociation by attaching weakly bound “messenger” atoms or molecules (H₂, N₂, Ne) to cluster ions.⁵² It is now more common to attach rare gas (RG) atoms, and many groups have employed this method to study molecular ions.^{53–56}

Our group and others have used tagging to study more strongly bound metal ion–molecular complexes.^{32–40,44} Tagged complexes have lower binding energies than the corresponding pure complexes and are therefore easier to dissociate. Following excitation of the C–H stretches, energy is transferred to the Ni⁺–RG coordinate, and the tagged complexes dissociate by losing one or more rare gas atoms. Because the rare gas atoms are most likely bound to the metal ion and do not interact strongly with the acetylene chromophore, the acetylene vibrations are not expected to be strongly perturbed by the tagging. The IRPD action spectra of the mixed complexes therefore provide the best possible approximation to the IR absorption spectra of the corresponding pure species. However, the exact structures of these complexes and the degree of interaction/perturbation on their spectra are important issues that we investigate below with DFT calculations.

1. Ni⁺(C₂H₂). Figure 2 shows the IRPD spectra of the Ni⁺–(C₂H₂) complexes with neon or argon rare gas atoms attached. Each spectrum was acquired in the mass channel that corresponds to the loss of a single rare gas atom. All of the spectra have features to the red of the free acetylene modes (asymmetric stretch, 3289 cm^{−1}; symmetric stretch, 3374 cm^{−1}),⁴⁵ consistent with the DCD model. Ni⁺(C₂H₂)Ar (not shown) is difficult to dissociate, leading to a broad spectrum with poor signal-to-noise

(50) Cotton, F. A.; Wilkinson, G. *Advanced Inorganic Chemistry*, 6th ed.; John Wiley & Sons: New York, 1999.

(51) MacBeth, C. E.; Thomas, J. C.; Betley, T. A.; Peters, J. C. *Inorg. Chem.* **2004**, *43*, 4645.

(52) (a) Okumura, M.; Yeh, L. I.; Lee, Y. T. *J. Chem. Phys.* **1985**, *83*, 3705. (b) Okumura, M.; Yeh, L. I.; Lee, Y. T. *J. Chem. Phys.* **1988**, *88*, 79. (c) Okumura, M.; Yeh, L. I.; Myers, J. D.; Lee, Y. T. *J. Phys. Chem.* **1990**, *94*, 3416.

(53) (a) Meuwly, M.; Nizkorodov, S. A.; Maier, J. P.; Bieske, E. J. *J. Chem. Phys.* **1996**, *104*, 3876. (b) Dopfer, O.; Roth, D.; Maier, J. P. *J. Phys. Chem. A* **2000**, *104*, 11702. (c) Bieske, E. J.; Dopfer, O. *Chem. Rev.* **2000**, *100*, 3963. (d) Meuwly, M.; Nizkorodov, S. A.; Maier, J. P.; Bieske, E. J. *J. Chem. Phys.* **1996**, *104*, 3876. (e) Bieske, E. J.; Dopfer, O. *Chem. Rev.* **2000**, *100*, 3963. (f) Dopfer, O.; Roth, D.; Maier, J. P. *J. Phys. Chem. A* **2000**, *104*, 11702. (g) Dopfer, O.; Roth, D.; Maier, J. P. *J. Chem. Phys.* **2001**, *114*, 7081. (h) Linnartz, H.; Verdes, D.; Maier, J. P. *Science* **2002**, *297*, 1166.

(54) (a) Bailey, C. G.; Kim, J.; Dessent, C. E. H.; Johnson, M. A. *Chem. Phys. Lett.* **1997**, *269*, 122. (b) Aoyotte, P.; Bailey, C. G.; Kim, J.; Johnson, M. A. *J. Chem. Phys.* **1998**, *108*, 444. (c) Aoyotte, P.; Weddle, G. H.; Kim, J.; Johnson, M. A. *J. Am. Chem. Soc.* **1998**, *120*, 12361. (d) Corcelli, S. A.; Kelley, J. A.; Tully, J. C.; Johnson, M. A. *J. Phys. Chem. A* **2002**, *106*, 4872. (e) Corcelli, S. A.; Kelley, J. A.; Tully, J. C.; Johnson, M. A. *J. Phys. Chem. A* **2002**, *106*, 4872. (f) Robertson, W. H.; Johnson, M. A. *Annu. Rev. Phys. Chem.* **2003**, *54*, 173. (g) Hammer, N. I.; Shin, J.-W.; Headrick, J. M.; Diken, E. G.; Roscoli, J. R.; Weddle, G. H.; Johnson, M. A. *Science* **2004**, *306*, 675.

(55) Satink, R. G.; Piest, H.; von Helden, G.; Meijer, G. *J. Chem. Phys.* **1999**, *111*, 10750.

(56) Pino, T.; Boudin, N.; Brechignac, P. *J. Chem. Phys.* **1999**, *111*, 7337.

(48) Alberts, I. L.; Rowlands, T. W.; Handy, N. C. *J. Chem. Phys.* **1988**, *88*, 3811.

(49) (a) Fischer, G.; Miller, R. E.; Vohralik, P. F.; Watts, R. O. *J. Chem. Phys.* **1985**, *83*, 1471. (b) Miller, R. E.; Vohralik, P. F.; Watts, R. O. *J. Chem. Phys.* **1984**, *80*, 5453.

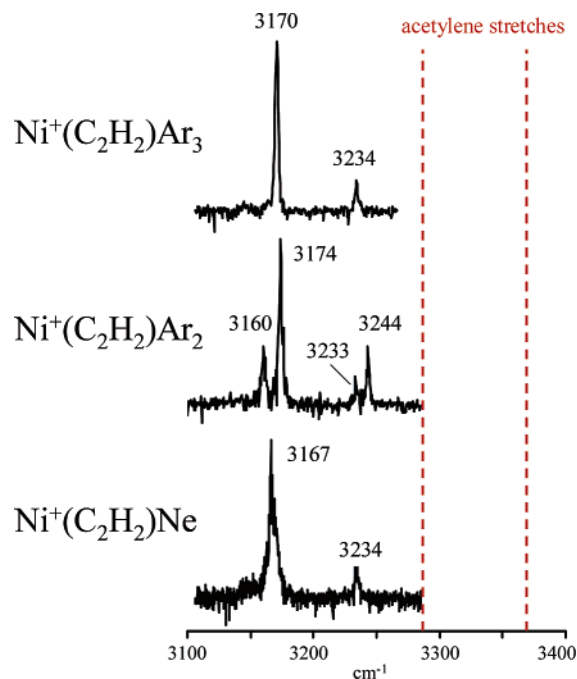


Figure 2. IRPD spectra of the $\text{Ni}^+(\text{C}_2\text{H}_2)$ complexes tagged with various rare gas atoms in the $3100\text{--}3300\text{ cm}^{-1}$ region.

ratio. The poor fragmentation of this complex is consistent with its marginal fragmentation energetics. Both theory⁵⁷ and experiment⁵⁸ agree that the $\text{Ni}^+\text{--Ar}$ diatomic has a dissociation energy of about 12 kcal/mol ($\sim 4000\text{ cm}^{-1}$). If the $\text{Ni}^+\text{--Ar}$ bond strength in the $\text{Ni}^+(\text{C}_2\text{H}_2)\text{Ar}$ complex is close to this value, one photon cannot dissociate this complex near 3200 cm^{-1} . Attaching a second argon is expected to lower the $\text{Ni}^+\text{--Ar}$ per-atom bond strength, and this increases the photodissociation efficiency. The middle trace shows the IRPD spectrum of the monoacetylene complex tagged with two argons. Two intense bands are observed at $3174/3244\text{ cm}^{-1}$, and a weak pair of peaks appear at $3160/3233\text{ cm}^{-1}$. When a third argon is added to this complex, the two doublets collapse to a single pair of resonances at 3170 and 3234 cm^{-1} , as can be seen in the upper trace of Figure 2. To acquire a high-quality spectrum of $\text{Ni}^+\text{--C}_2\text{H}_2$ with a single messenger atom, we attach neon. The $\text{Ni}^+\text{--Ne}$ bond is calculated to be 3.4 kcal/mol ($\sim 1190\text{ cm}^{-1}$),⁵⁷ and experiment puts it at 2.4 kcal/mol ($\sim 840\text{ cm}^{-1}$).⁵⁹ Absorption of a single photon near 3200 cm^{-1} should dissociate the $\text{Ni}^+(\text{C}_2\text{H}_2)\text{Ne}$ complex. Consistent with this, the neon-tagged complex does dissociate efficiently, yielding a spectrum with two features at 3167 and 3234 cm^{-1} . The line widths of the $\text{Ni}^+(\text{C}_2\text{H}_2)\text{Ar}_2$ and $\text{Ni}^+(\text{C}_2\text{H}_2)\text{Ar}_3$ bands are $3\text{--}4\text{ cm}^{-1}$, while those for the $\text{Ni}^+(\text{C}_2\text{H}_2)\text{Ne}$ bands are about 5 cm^{-1} , with slight asymmetry on the blue side. It is conceivable that the additional width in the $\text{Ni}^+(\text{C}_2\text{H}_2)\text{Ne}$ spectrum is partly due to the rotational contours of the bands, but the rotational constants of the $\text{Ni}^+(\text{C}_2\text{H}_2)\text{Ar}_2$ and $\text{Ni}^+(\text{C}_2\text{H}_2)\text{Ar}_3$ complexes are too small for such structure to be resolved.

All of the spectra in Figure 2 have resonances near 3170 and 3240 cm^{-1} . The bands are therefore assigned respectively to

- (57) Partridge, H.; Bauschlicher, C. W.; Langhoff, S. R. *J. Phys. Chem.* **1992**, *96*, 5350.
 (58) (a) Lessen, D. E.; Asher, R. L.; Brucat, P. J. *Adv. Metal Semicond. Clusters* **1993**, *1*, 267. (b) Lessen, D. E.; Brucat, P. J. *Chem. Phys. Lett.* **1988**, *152*, 473.
 (59) Kemper, P. R.; Hsu, M.-T.; Bowers, M. T. *J. Phys. Chem.* **1991**, *95*, 10600.

the asymmetric and symmetric C–H stretches of the acetylene ligand within these cation complexes. The symmetric stretch of free acetylene is not infrared active, but once this ligand is bound to the metal ion, the symmetry of the entire complex must be considered and this mode becomes active. As described below, theory shows that the hydrogens bend slightly away from the cation, and this distortion gives the symmetric stretch a small IR intensity. It is therefore understandable that we detect resonances assigned to the symmetric stretch. The spectrum measured for $\text{Ni}^+(\text{C}_2\text{H}_2)\text{Ar}_2$ is hard to understand. Only two C–H stretches are expected here, but four bands are observed. The weak signals are red-shifted from the intense bands, but they are still in the acetylene C–H stretch region. This suggests that there are two closely related kinds of molecules present in the $\text{Ni}^+(\text{C}_2\text{H}_2)\text{Ar}_2$ mass channel. Impurities can be ruled out by the mass selection of the parent ion and the mass analysis (loss of argon) in the fragmentation process. It therefore seems that some sort of isomeric species is present only when two argons are attached to this complex.

There are several ways in which isomers might be formed for the $\text{Ni}^+(\text{C}_2\text{H}_2)\text{Ar}_2$ complex. It is conceivable that insertion chemistry has occurred, and insertion products would have the same mass as the unreacted complex and could not be distinguished by our mass selection. However, it is not clear why insertion would be seen only for the diargon complex and not for the neon or triargon species. Unlike the early transition metals, nickel cation is not expected to insert into small hydrocarbons,^{3,4,6–8} and indeed no fragmentation products are observed in our mass spectra. Also, any insertion complexes would not likely have acetylenic C–H stretches ($3200\text{--}3400\text{ cm}^{-1}$), and so we can safely rule out isomers generated from insertion chemistry. Another possibility is the presence of isomers with argon attached in different positions in the complex. Similar isomers were recently identified in our study of $\text{M}^+(\text{H}_2\text{O})\text{Ar}_n$ ($\text{M} = \text{Fe}, \text{Mg}$) complexes, where the OH groups competed with the metal ion for the argon binding.³⁹ In that work, an argon attached to water caused a significant red-shift of the OH stretching frequencies due to an OH–Ar form of weak hydrogen bonding. A similar red-shift is possible here if argon binds to an acetylene CH group instead of to the nickel cation, and this could account for the weaker red-shifted peaks observed in the $\text{Ni}^+(\text{C}_2\text{H}_2)\text{Ar}_2$ spectrum. The strong bands might be from isomers where both argon atoms are attached directly to the metal, whereas the weaker signals could come from isomers with at least one argon attached to acetylene. We therefore turn to theory in order to investigate this possibility and to aid us in our interpretation of this spectrum and those for the other complexes.

DFT calculations were therefore carried out on both the pure acetylene complexes, $\text{Ni}^+(\text{C}_2\text{H}_2)_n$, for $n = 1\text{--}4$, and for those tagged with argon ($n = 1\text{--}3$) or neon ($n = 1$). The essential results of these calculations are presented in Tables 1 and 2, while a full account is presented in the Supporting Information. Geometry optimizations were performed at the B3LYP level with both the 6-31G* and the 6-311+G** basis sets. Dissociation energies and structural parameters for these complexes with the higher basis set are listed in Table 1, whereas the corresponding vibrations for these complexes in the C–H stretch region are presented in Table 2. The lowest energy structures calculated are shown in Figure 3 for the pure $\text{Ni}^+(\text{C}_2\text{H}_2)_{1\text{--}4}$

Table 1. B3LYP/6-311+G** Energetics and Structural Data for Ni⁺(C₂H₂)_n(RG)_m Complexes

complex	BE ^a	D _e ^b	M ⁺ -L (Å) ^c	M ⁺ -RG (Å)	C-C (Å)	∠CCH (deg)
Ni ⁺ (C ₂ H ₂)						
² B ₁ (C _{2v})	47.0	47.0	1.867	-	1.234	165.8
² A ₁ (C _{2v})	46.6	46.6	1.947	-	1.228	166.8
Ni ⁺ (C ₂ H ₂)Ne						
² A'' (C _s)	49.9	2.8 (Ne) 48.0 (C ₂ H ₂)	1.896	2.356	1.233	166.0, 165.8
² A' (C _s)	49.6	2.6 (Ne) 47.7 (C ₂ H ₂)	1.946	2.325	1.228	166.9, 167.1
Ni ⁺ (C ₂ H ₂)Ar						
² B ₁ (C _{2v})	56.6	9.5 (Ar) 47.4 (C ₂ H ₂)	1.894	2.416	1.232	166.0
² A ₁ (C _{2v})	56.4	9.7 (Ar) 47.2 (C ₂ H ₂)	1.948	2.407	1.227	167.0
Ni ⁺ (C ₂ H ₂)Ar ₂						
² B ₁ (C _{2v})	60.4	3.8 (Ar) 41.2 (C ₂ H ₂)	1.917	2.531	1.230	166.1
² A ₁ (C _{2v})	57.1	1.7 (Ar) 37.9 (C ₂ H ₂)	1.916	2.621	1.226	166.9
² A'' (C _s) (Ar on CH)	57.0	13.5 (Ni ⁺ -Ar) 0.4 (CH-Ar) 37.7 (C ₂ H ₂)	1.895	2.416	1.232	166.3
Ni ⁺ (C ₂ H ₂)Ar ₃						
² A' (C _s)	61.6	1.3 (Ar) 33.4 (C ₂ H ₂)	1.916	2.600, 2.670	1.232	164.7
² A'' (C _s)	59.4	0.9 (Ar) 31.2 (C ₂ H ₂)	1.918	2.598, 3.163	1.231	164.9
² A'' (C _s) (Ar on CH)	60.8	3.9 (Ni ⁺ -Ar) 0.4 (CH-Ar) 32.6 (C ₂ H ₂)	1.917	2.532	1.230	166.1, 166.3
Ni ⁺ (C ₂ H ₂) ₂						
² A ₂ (C _{2v})	85.5	38.4 (C ₂ H ₂)	1.989		1.221	170.3, 169.3
² B ₂ (D _{2d})	84.0	36.9 (C ₂ H ₂)	1.989		1.222	168.4
Ni ⁺ (C ₂ H ₂) ₂ Ar						
² A ₂ (C _{2v})	85.8	29.2 (C ₂ H ₂) 0.3 (Ar)	1.977	3.283	1.233	167.6, 169.2
² A ₁ (C _{2v})	83.6	27.0 (C ₂ H ₂) 0.1 (Ar)	2.037	4.374	1.218	170.3, 170.4
² A' (C _s) (Ar on CH)	84.4	27.8 (C ₂ H ₂) 0.4 (Ar)	1.989, 1.988		1.222	168.3, 168.5 168.4
Ni ⁺ (C ₂ H ₂) ₃						
² A' (C _s)	101.6	16.1 (C ₂ H ₂)	2.091, 2.023	-	1.216 1.221	169.4, 170.2 167.7
Ni ⁺ (C ₂ H ₂) ₃ Ar						
² A' (C _s)	101.8	15.9 (C ₂ H ₂) 0.2 (Ar)	2.092, 2.024	4.159	1.216 1.220	169.5, 170.4 167.8
² A' (C _s) (Ar on CH)	101.7	15.9 (C ₂ H ₂) 0.2 (Ar)	2.103, 2.102 2.034		1.215 1.219	170.9, 168.8
Ni ⁺ (C ₂ H ₂) ₄						
² A' (C _s)	105.5	4.9 (C ₂ H ₂)	2.135, 2.105 2.436		1.217 1.219 1.205	166.2, 165.7 165.4, 165.4 174.6, 175.0

^a Binding energy of the complex in kcal/mol relative to Ni⁺ and separated ligands. ^b Dissociation energy in kcal/mol for removal of the ligand indicated. ^c Distance from the metal ion to the center of the C≡C bond.

complexes. The structures for tagged complexes are only slightly different from those without tagging. Key structural details are also presented for these complexes in the tables, and their structures are shown in the Supporting Information.

DFT finds that the first acetylene binds to the nickel cation to form a ²B₁ π-complex with C_{2v} symmetry, consistent with the previous theoretical studies on the Ni⁺(C₂H₂) complex.^{14,17} An excited state with ²A₁ symmetry is calculated by DFT to lie ~1.5 kcal/mol higher in energy, whereas previous modified coupled pair (MCP) calculations found these two states to be isoenergetic.¹⁴ The binding interaction causes two main effects, both of which are consistent with the DCD model. The C≡C bond is lengthened relative to that calculated at the same level for the free acetylene molecule (1.234 versus 1.199 Å; see Supporting Information), and the hydrogen atoms are pushed

away from the C≡C axis (∠CCH = 165.8°) to reduce repulsion from the nickel cation. The weakening of the binding in the acetylene moiety causes its stretching fundamentals to shift to lower energy, and the bending of the hydrogen atoms causes the symmetric C-H stretch to become weakly infrared active. The C-H stretches in Ni⁺(C₂H₂) are predicted to red-shift by ~135 cm⁻¹ for both the asymmetric and symmetric modes.

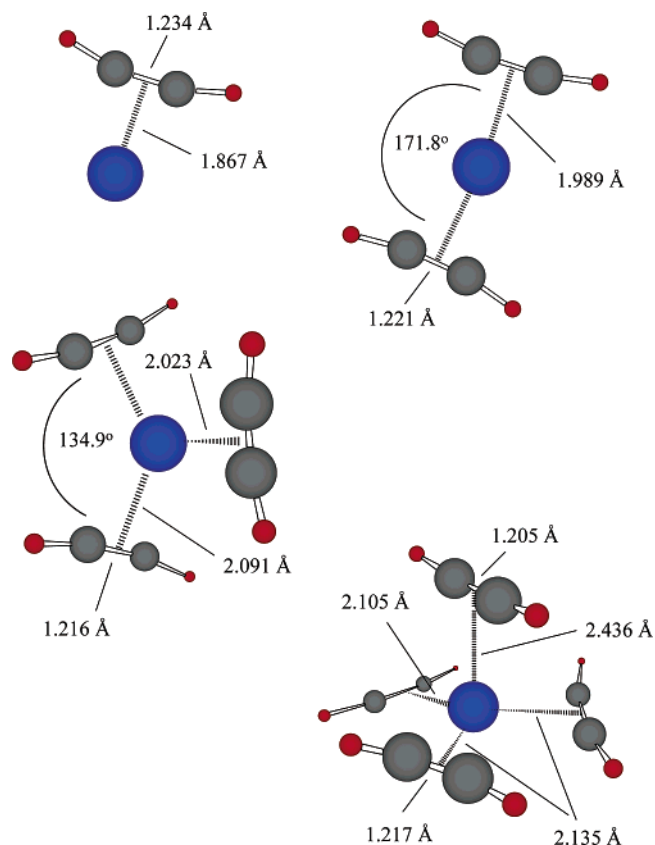
Neon attaches to the nickel cation on the opposite side from the acetylene molecule, slightly removed (~5°) from the C₂ axis. Presumably, this slight asymmetry results from a Jahn-Teller interaction. The electronic configuration of Ni⁺ is d⁹, and the cation often Jahn-Teller distorts. Therefore, the Ni⁺(C₂H₂)Ne complex has C_s rather than C_{2v} symmetry. Attempts to constrain the molecule to the C_{2v} point group failed. The ground state is ²A'', and an excited ²A' state lies only 0.3 kcal/mol higher in

Table 2. C–H Frequencies (cm^{-1}) (B3LYP/6-311+G**; 0.96 scaled) and Intensities (km/mol) Compared to the Experiment

complex/state	theory	experiment
$\text{Ni}^+(\text{C}_2\text{H}_2)$		
$^2\text{B}_1 (C_{2v})$	3156 (232), 3240 (27)	
$^2\text{A}_1 (C_{2v})$	3165 (225), 3251 (26)	
$\text{Ni}^+(\text{C}_2\text{H}_2)\text{Ar}$		
$^2\text{B}_1 (C_{2v})$	3163 (214), 3247 (34)	
$^2\text{A}_1 (C_{2v})$	3172 (209), 3259 (33)	
$\text{Ni}^+(\text{C}_2\text{H}_2)\text{Ar}_2$		
$^2\text{B}_1 (C_{2v})$	3170 (195), 3255 (35)	3160, 3233
$^2\text{A}_1 (C_{2v})$	3177 (196), 3264 (34)	3174, 3244
$^2\text{A}'' (C_s)$ (Ar on CH)	3155 (303), 3241 (42)	
$\text{Ni}^+(\text{C}_2\text{H}_2)\text{Ar}_3$		
$^2\text{A}' (C_s)$	3173 (173), 3255 (38)	3170, 3234
$^2\text{A}'' (C_s)$	3172 (177), 3254 (40)	
$^2\text{A}' (C_s)$ (Ar on CH)	3163 (277), 3250 (46)	
$\text{Ni}^+(\text{C}_2\text{H}_2)\text{Ne}$		
$^2\text{A}'' (C_s)$	3159 (227), 3243 (28)	3167, 3234
$^2\text{A}' (C_s)$	3168 (220), 3254 (28)	
$\text{Ni}^+(\text{C}_2\text{H}_2)_2$		
$^2\text{A}_2 (C_{2v})$	3185 (4), 3186 (426), 3275 (84), 3279 (1)	
$^2\text{B}_2 (D_{2d})$	3185 (208), 3185 (208), 3275 (0), 3277 (39)	
$\text{Ni}^+(\text{C}_2\text{H}_2)_2\text{Ar}$		
$^2\text{A}_2 (C_{2v})$	3188 (25), 3190 (360), 3276 (80), 3280 (8)	3176, 3185, 3196, 3262
$^2\text{A}_1 (C_{2v})$	3193 (0), 3194 (422), 3284 (76), 3288 (0)	
$^2\text{A}' (C_s)$ (Ar on CH)	3180 (268), 3185 (207), 3273 (15), 3277 (29)	
$\text{Ni}^+(\text{C}_2\text{H}_2)_3$		
$^2\text{A}' (C_s)$	3211 (9), 3213 (313), 3214 (157), 3300 (45), 3302 (50), 3305 (10)	
$\text{Ni}^+(\text{C}_2\text{H}_2)_3\text{Ar}$		
$^2\text{A}' (C_s)$	3213 (4), 3214 (157), 3215 (316), 3301 (43), 3303 (47), 3306 (10)	3195, 3206, 3216, 3270, 3287
$^2\text{A}' (C_s)$ (Ar on CH)	3212 (0), 3213 (184), 3213 (351), 3301 (51), 3303 (46)	
$\text{Ni}^+(\text{C}_2\text{H}_2)_4$		
$^2\text{A}' (C_s)$	3229 (39), 3235 (120), 3237 (146), 3258 (135), 3314 (50), 3320 (56), 3324 (11), 3356 (8)	3228, 3252, 3298, 3338

energy, with properties very similar to those of the ground state. Attaching neon to $\text{Ni}^+(\text{C}_2\text{H}_2)$ induces only the slightest change on the acetylene subunit, as summarized in Table 1. The $\text{C}\equiv\text{C}$ distance and CCH angle are essentially unchanged, but the Ni^+ –acetylene distance increases slightly (from 1.867 to 1.896 Å). Interestingly, the Ni^+ – (C_2H_2) dissociation energy actually increases slightly when Ne is added to the complex (from 47.0 to 48.0 kcal/mol). It is not clear if this small difference is significant, as DFT has problems with energetics, especially when weak bonding is present.^{16,60} In the IR spectrum, the C–H stretches in the neon-tagged complex are predicted to shift back toward the free acetylene frequencies by only 3 cm^{-1} relative to the values calculated for $\text{Ni}^+(\text{C}_2\text{H}_2)$.

Unlike neon, argon attaches to the nickel cation on the C_2 axis, and the $\text{Ni}^+(\text{C}_2\text{H}_2)\text{Ar}$ complex has C_{2v} symmetry. We identified an isomer with argon binding to the C–H of acetylene, but this lies at much higher energy (see Supporting Information). As seen for the neon complex, the geometry of the acetylene is essentially unchanged by the presence of the rare gas, but the Ni^+ –acetylene bond distance increases slightly. DFT predicts that the argon causes the C–H resonances to shift back toward the free molecule vibrations by $\sim 6 \text{ cm}^{-1}$ compared to $\text{Ni}^+(\text{C}_2\text{H}_2)$. In $\text{Ni}^+(\text{C}_2\text{H}_2)\text{Ar}_2$, the possibility of structural isomers arises depending on where the second argon attaches to the cluster. We have investigated all possible isomers of this type with DFT (see Supporting Information). The most stable one has the second argon binding on the same side of nickel as the

**Figure 3.** Theoretical structures for the $\text{Ni}^+(\text{C}_2\text{H}_2)_n$ ($n = 1-4$) complexes computed with DFT/B3LYP and the 6-311+G** basis set.(60) Cramer, C. J. *Essentials of Computational Chemistry*; John Wiley & Sons: Chichester, England, 2002.

first, producing an Ar–Ni⁺–Ar angle of 89.4°. The structure of acetylene is unchanged, but the Ni⁺–acetylene bond distance increases slightly again with the addition of the second rare gas. The second argon is predicted to cause an *additional* 8 cm⁻¹ spectral shift (~14 cm⁻¹ total shift) toward the free molecule vibrations relative to those in Ni⁺(C₂H₂). Isomers of Ni⁺(C₂H₂)–Ar₂ are also identified with one or both of the argons binding on the C–H of acetylene. The latter lies at much higher energy, but the former is predicted to lie only 3.4 kcal/mol above the isomer with both argons on the metal. Isomeric structures are also possible for Ni⁺(C₂H₂)Ar₃ (see Supporting Information). The most stable of these also has all three Ar atoms bound to Ni⁺ on the same side, opposite the acetylene, and the isomer with one argon on C–H is also found at low energy. Attachment of argon to Ni⁺ produces essentially no change in the acetylene structure. The binding energy of the acetylene increases very slightly when one argon is added to the Ni⁺(C₂H₂) complex, but additional argons causes the Ni⁺–acetylene bond to gradually weaken as the binding interaction is distributed over more ligands. A significant drop in this binding is evident between the second and third argons as the coordination around the nickel becomes more nearly filled. The addition of more argon has only a small effect on the C–H frequencies. All the argon complexes have low-lying excited states, just like the untagged and the neon-tagged system.

The spectra calculated in the C–H stretching region compare favorably with those that we measure. Unfortunately, we cannot measure any spectrum for Ni⁺(C₂H₂) without tagging. For the tagged systems, the simplest spectra are those for the neon and Ar₃ complexes. The experimental band positions for Ni⁺(C₂H₂)–Ne at 3167 and 3234 cm⁻¹ compare favorably to the values predicted at 3159 and 3243 cm⁻¹. The Ni⁺(C₂H₂)Ar₃ complex also has only two bands in the C–H region, at 3170 and 3234 cm⁻¹. These are in good agreement with those predicted for the ²A' ground state of the isomer with all argons attached to the metal at 3173 and 3255 cm⁻¹. As noted above, the Ni⁺(C₂H₂)Ar₂ spectrum has doublets at 3160/3174 and 3233/3244 cm⁻¹, with the higher frequency band for each doublet having roughly twice the intensity of the lower frequency member. These can be compared to the calculated asymmetric and symmetric resonances for the ²B₁ ground state of the isomer with both argons attached to the metal at 3170 and 3255 cm⁻¹. The more intense peaks in each doublet agree reasonably well with the predicted band positions, but we have still not explained the weaker doublet members lying at lower frequencies.

Our calculations provide a possible interpretation for these additional bands in the Ni⁺(C₂H₂)Ar₂ spectrum. As noted above, an isomer with one argon attached to the cation and one attached to the C–H of acetylene is identified at low energy in the calculations, lying 3.4 kcal/mol above the lowest energy structure. As indicated in the tables, this C_s isomer has C–H vibrations that are predicted to be shifted 10–15 cm⁻¹ to the red from the vibrations of the most stable isomer. This red-shift arises because argon binding to a C–H has an effect like that seen for hydrogen bonding in water clusters, which also results in red-shifted hydrogen stretch vibrations. We have recently described in detail how argon binding on the OH of water in Mg⁺(H₂O) complexes causes a similar red-shift of the O–H stretches.^{39c} In the present system, a small concentration of such an isomer would be enough to explain the weaker pair

of red-shifted bands seen for Ni⁺(C₂H₂)Ar₂. However, the calculations also suggest another possible mechanism to explain the doublet bands seen for this cluster. Ni⁺ has a low-lying ²D_{3/2} state that is 4.3 kcal/mol (~1500 cm⁻¹) above the ²D_{5/2} ground state.⁶¹ This gives rise to the ²A₁ excited state calculated by DFT for the Ni⁺(C₂H₂) complex, which lies close in energy to the calculated ²B₁ ground state (~3.3 kcal/mol). The calculations show that the energy difference between the ²A₁ and ²B₁ states (or states with other symmetries corresponding to these) is also small in all the tagged complexes. In Ni⁺(C₂H₂)Ar₂, this energy difference is 3.3 kcal/mol, and similar values are found for the other *n* = 1 complexes here. DFT calculations are by no means quantitative in this situation,^{16,60} and we can only say for sure that there are low-lying states for all of these complexes. It is therefore conceivable that both the ground and low-lying states are populated for all of these complexes, and this could give rise to spectra that represent a superposition of bands for both states. Our calculations find that the C–H frequency differences between the ground and excited states are 7–9 cm⁻¹ for the Ar₂ complex, which then makes this another possible assignment for the doublet structure. It is apparent, then, that either a minor population of an isomer with argon on C–H or an excited electronic state could explain the extra bands in the Ni⁺(C₂H₂)–Ar₂ spectrum. Unfortunately, we cannot distinguish between these two possibilities.

It is actually surprising that we only see additional structure in the Ni⁺(C₂H₂)Ar₂ spectrum and none in the corresponding neon- or Ar₃-tagged spectra. All of these species should have the same low-lying excited states, and several isomeric structures are predicted for the Ar₃ complex. However, none of the calculated energy or frequency differences in these systems are expected to be perfectly quantitative, and we cannot use the calculations to make detailed interpretations. We can only conclude that some combination of factors works out to produce a composite spectrum for Ni⁺(C₂H₂)Ar₂. In the cases of Ni⁺(C₂H₂)Ne and Ni⁺(C₂H₂)Ar₃, either the two states or isomers are not populated appreciably or their frequency differences are too small to resolve.

2. Ni⁺(C₂H₂)₂. Attaching a single argon atom was sufficient to acquire the vibrational spectrum of the Ni⁺(C₂H₂)₂ complex. We have therefore performed calculations only for the untagged Ni⁺(C₂H₂)₂ complex and for that tagged with one argon. As we found for the *n* = 1 complex with neon, the ²A₂ ground state of the *n* = 2 complex does not have the two ligands exactly opposite each other. Instead, they are puckered to one side, with an angle of 171.8° between the two Ni⁺–acetylene bonds, forming a C_{2v} structure. The system is still planar, with Ni⁺–acetylene bond distances (1.989 Å) slightly longer than in the *n* = 1 complex (1.867 Å). Although the Ni⁺–acetylene bond energy increased slightly when we added either neon or argon to the *n* = 1 complex, the average over the two ligand bonds is less than in the *n* = 1 system. The geometries of each acetylene here are quite close to that in the *n* = 1 complex, although the two CCH angles are slightly different due to H–H repulsion. We also find an isomer with a D_{2d} staggered-ligand configuration, lying just 1.5 kcal/mol higher than the C_{2v} structure. Argon binds equally well in both of these isomeric structures, inducing only slight structural changes and energy differences. We investigated the electronically excited state only for the C_{2v}

(61) Sugar, J.; Corliss, C. *J. Phys. Chem. Ref. Data* **1985**, 14 (Suppl.), 1.

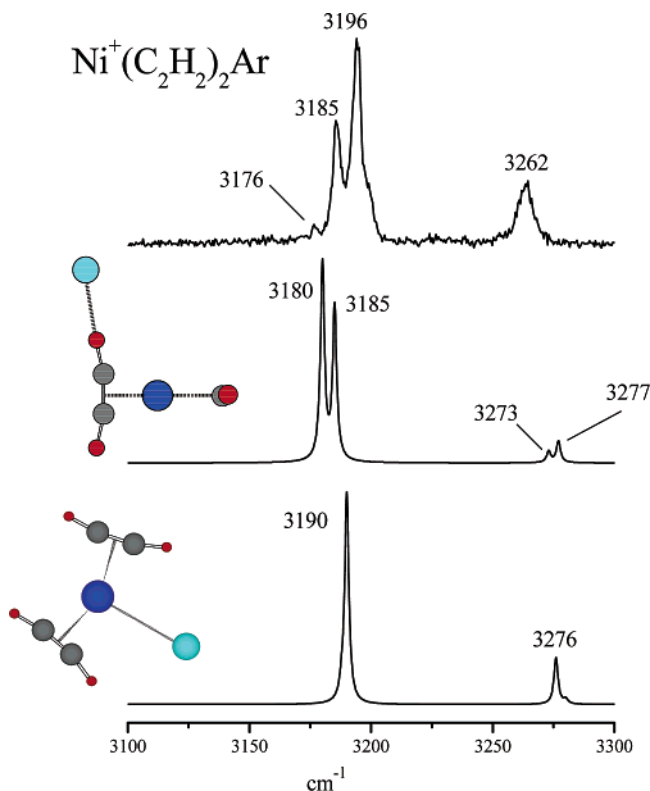


Figure 4. IRPD spectrum of $\text{Ni}^+(\text{C}_2\text{H}_2)_2\text{Ar}$ compared to the predictions of theory. The center trace corresponds to an isomer with argon on C–H, while the lower trace is the spectrum for the most stable isomer found with argon bound to Ni^+ . Neither agrees perfectly with the experiment.

isomer tagged with argon, and this is predicted to lie within about 2.0 kcal/mol of the ground state. It is therefore conceivable that the spectrum of this complex could have contributions from isomeric structures and the low-lying excited state.

Figure 4 shows the IRPD spectrum of $\text{Ni}^+(\text{C}_2\text{H}_2)_2\text{Ar}$ and how it compares to the frequencies of the two isomeric structures calculated for this complex. The experimental spectrum has reproducible strong bands at 3185, 3196, and 3262 cm^{-1} and a weak band at 3176 cm^{-1} . The observation of three strong bands in the C–H stretch region is somewhat surprising. If the two acetylenes are coplanar and attached to the cation on opposite sides in a D_{2h} structure, the $\text{Ni}^+(\text{C}_2\text{H}_2)_2$ complex would have four C–H vibrations corresponding to in-phase and out-of-phase motions of the symmetric and asymmetric C–H stretches. Only two of these would be IR active: the out-of-phase symmetric stretch and the in-phase asymmetric stretch. Thus, although such a D_{2h} structure is not predicted by theory, it would have only two bands, which is not consistent with the spectrum. As shown in the figure, the tagged C_{2v} structure is also predicted to have essentially a two-peak spectrum. Because its symmetry is lower than the D_{2h} configuration, all four C–H stretches are actually IR active, and their frequencies are predicted at 3188, 3190, 3276, and 3280 cm^{-1} . However, these pairs of peaks are not resolved when plotted at the 2 cm^{-1} resolution typical of our experiment. Table 2 contains these calculated band positions and their infrared oscillator strengths. The bands measured at 3196 and 3262 cm^{-1} compare favorably to the theoretical frequencies at 3190 and 3276 cm^{-1} . However, the experimental spectrum also contains a relatively intense peak at 3185 cm^{-1} and a weak but reproducible feature at 3176 cm^{-1} , which are not explained by this lowest energy structure. It is conceivable

that the $n = 2$ complex adopts a structure that is less symmetric than the one calculated by DFT. A more distorted geometry might lift the degeneracy of the two band pairs, giving more multiplet structure. Figure 4 also shows the spectrum calculated for the higher energy D_{2d} isomer. In this isomer, the two acetylenes effectively block the access to the metal ion, and the lowest energy configuration places the argon on the C–H of one acetylene. As noted above, such a binding configuration induces a red-shift on the C–H vibrations of that ligand. As can be seen in the figure, the spectrum for this isomer has multiplet structure in the asymmetric stretch region, which is enough to account for the positions of the two main bands that we measure here. However, the relative intensity of the multiplet predicted at 3180/3185 cm^{-1} is not the same as that measured at 3185/3196 cm^{-1} , and there is no peak matching up with the minor feature at 3176 cm^{-1} . Except for these inconsistencies, it is possible that the D_{2d} isomer alone explains the spectrum. Both the C_{2v} and D_{2d} isomers should have low-lying excited states, as we have discussed above, but the frequencies that we calculated for the C_{2v} isomer were essentially the same as those for the ground state. However, because of uncertainties in all the calculated frequencies and IR intensities, it is really impossible to rule out contributions to the multiplet structure seen here from either isomeric structure or from their corresponding low-lying excited states. Some superposition of these possibilities apparently produces the multiplet structure that is seen.

3. $\text{Ni}^+(\text{C}_2\text{H}_2)_3$. Our calculations for the $\text{Ni}^+(\text{C}_2\text{H}_2)_3$ complex produced only one isomeric structure with all three acetylene ligands π -bonded to the nickel, which is shown in Figure 3. This structure has two equivalent acetylenes and a third unique one in the structure. It is convenient to view this as built on the C_{2v} isomer of the $n = 2$ complex. However, unlike the $n = 2$ isomer, the metal ion in the $n = 3$ complex is not in the same plane as the two puckered acetylenes. The third acetylene binds almost opposite the other two, but it is rotated with respect to them. The nickel cation is located near the plane defined by the three center-of-mass points of the acetylenes. To aid in defining this structure, we give different views of it in the Supporting Information.

The spectrum predicted for the $n = 3$ complex is quite interesting. Six IR-active C–H stretches are identified by DFT for $\text{Ni}^+(\text{C}_2\text{H}_2)_3$. In the tagged complex, the argon attaches in a position approximately opposite the three acetylenes, so that the overall configuration of the four ligands is nearly tetrahedral. Figure 5 displays the spectrum for $\text{Ni}^+(\text{C}_2\text{H}_2)_3\text{Ar}$ and how it compares to the predicted spectrum calculated using different basis sets. Theoretical frequencies have been scaled by 0.96 and plotted at a 2 cm^{-1} resolution. As shown in the middle frame of the figure, the $n = 3$ complex calculated with the larger 6-311+G** basis set (used throughout the other studies reported here) produces a spectrum that has essentially only two bands at this resolution. This is not at all consistent with the experimental spectrum, which has two regions of signal, each split into multiplet structure. In the region of the asymmetric stretch, the experiment has three bands at 3195, 3206, and 3216 cm^{-1} , while in the region of the symmetric stretch there are two bands at 3270 and 3287 cm^{-1} . Again, as for the smaller complexes, we have to investigate other scenarios to explain the additional structure in this spectrum.

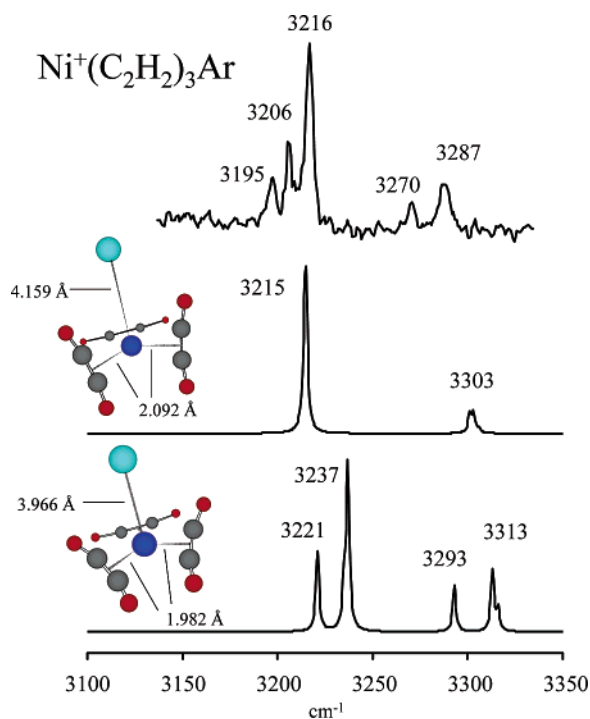


Figure 5. Figure 5. IRPD spectrum of $\text{Ni}^+(\text{C}_2\text{H}_2)_3\text{Ar}$ compared to the predictions of theory. The spectrum from the 6-311+ G^{**} calculation (center trace) is less consistent with the experiment, while that with the 6-31 G^* basis set (bottom trace) has more multiplet structure.

As we have seen for all these complexes so far, a low-lying excited electronic state is possible here. However, we have calculated the spectroscopy for this state and found that it does not differ appreciably from the spectrum for the ground state. Two main bands are predicted, but these alone are not enough to explain the number of multiplet peaks observed. As in the $n = 2$ complex, we also investigated isomeric structures with argon binding on an acetylene C–H instead of on the metal. The complexes with more ligands tend to have steric crowding, and such isomers become energetically competitive with those having the argon attached to the metal ion. Again, as described in the Supporting Information, an isomer with argon on C–H is also found for this complex, lying essentially at the same energy as the isomer with argon attached to the metal ion. However, the calculated spectra of these two isomers are the same within the 2 cm^{-1} resolution of the experiment, and so this does not explain the spectroscopy either.

A final odd occurrence for this complex is that the IR spectroscopy predicted varies substantially with the basis set employed. As we noted above, all of these complexes were studied with the smaller 6-31 G^* basis set before we employed the larger 6-311+ G^{**} basis. For all the other complexes, the spectra with these two basis sets were essentially identical, as expected. However, for the present $n = 3$ complex, this is not the case. The structures and spectra for the two basis sets are quite different, especially regarding the multiplets in the C–H stretch region. The lower spectrum in Figure 5 is that predicted with the smaller 6-31 G^* basis. There are three asymmetric-like modes at 3221, 3235, and 3237 cm^{-1} and three symmetric-like modes at 3293, 3313, and 3316 cm^{-1} calculated for $\text{Ni}^+(\text{C}_2\text{H}_2)_3\text{Ar}$ in the $^2A'$ electronic state. When plotted at a 2 cm^{-1} resolution, the theoretical spectrum is dominated by only four infrared bands: two in the asymmetric region and two in

the symmetric region. This certainly looks more like the experimental spectrum than the one predicted at the 6-311+ G^{**} level. However, even this spectrum does not account for all the peaks measured. We must then speculate that some combination of factors explains the spectrum, including perhaps some population in the low-lying excited state and/or the argon-on-CH isomer together with the ground state. Since DFT behaves in a strange way with different basis sets for this complex, it is also conceivable that the ground state alone has an IR spectrum with the multiplets measured, but this state is just not described adequately by the calculations.

4. $\text{Ni}^+(\text{C}_2\text{H}_2)_4$. Two isomeric structures were identified with DFT for the $n = 4$ complex. The first has all four acetylenes attached directly to the metal ion in a near-tetrahedral (C_4) arrangement, and the second is a “3+1” complex, where the fourth acetylene is attached in a van der Waals or weak hydrogen-bonding configuration interacting with two inner-sphere acetylene molecules. A square-planar structure was also considered, but these calculations failed to converge. In the same way seen for the $n = 1$ and 2 complexes, but different from the behavior for $n = 3$, significant changes are not observed when these structures were calculated with either the small or large basis sets. Therefore, the results presented here are from the 6-311+ G^{**} calculations. According to the computations, the isomers are nearly isoenergetic, with the “3+1” structure being more stable by only 1.0 kcal/mol. In both the four-coordinate and 3+1 structures, the binding energy of the last acetylene ligand is quite low (4.9 kcal/mol). The corresponding value calculated for the $n = 3$ complex is about 16 kcal/mol. It thus appears that there is a substantial drop in the binding energy between the third and fourth ligands. Consistent with the idea that four acetylenes saturate the coordination around the cation, we are not able to attach argon efficiently to the $n = 4$ complex. However, we are able to photodissociate this complex efficiently without the need for tagging. The spectrum shown for this complex in Figure 6, therefore, is recorded in the mass channel corresponding to the loss of one acetylene. Using the small amount of argon-tagged ions that we can produce, we have also measured this spectrum in the loss-of-argon channel. The spectrum measured this way is slightly sharper and has worse signal levels, but is otherwise the same as the nontagged spectrum.

Figure 6 shows the spectrum of $\text{Ni}^+(\text{C}_2\text{H}_2)_4$ and its comparison to the predicted spectra for the two theoretical structures. Harmonic frequencies have been scaled by 0.96 and plotted at a 10 cm^{-1} resolution for better comparison to the resolution of the experiment. The experimental spectrum for $\text{Ni}^+(\text{C}_2\text{H}_2)_4$ has three intense bands at 3228, 3252, and 3298 cm^{-1} and a weak but reproducible band at 3338 cm^{-1} . DFT predicts eight infrared active C–H vibrations for four-coordinate $\text{Ni}^+(\text{C}_2\text{H}_2)_4$ due to its lower symmetry, and their frequencies and intensities are summarized in Table 2. However, many of these vibrations overlap when plotted at the resolution of the experiment. For example, the asymmetric-like C–H resonances at 3229, 3235, and 3237 cm^{-1} appear as a single strong infrared band at 3236 cm^{-1} , as seen in the middle trace of the figure. Likewise, overlapping symmetric features at 3314, 3320, and 3324 cm^{-1} produce a broad band centered near 3318 cm^{-1} . Therefore, only four bands are apparent in the theoretical spectrum at the experimental resolution. As shown in the figure, the match

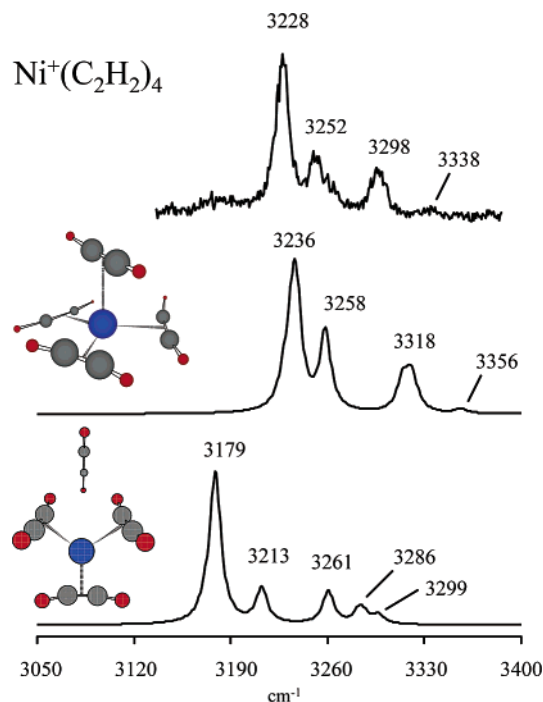


Figure 6. IRPD spectrum of $\text{Ni}^+(\text{C}_2\text{H}_2)_4$ as it compares to the four-coordinate and 3+1 isomers calculated.

between experiment and theory for the four-coordinate complex is quite good for both band positions and intensities. The lower trace of the figure shows the spectrum calculated for the 3+1 isomer. It also has several overlapping vibrations that merge to form broad bands at the experimental resolution. However, the most noticeable feature of this spectrum is the strong band at 3179 cm^{-1} . This band is shifted almost 50 cm^{-1} further to the red than anything measured in the experiment or predicted in the four-coordinate complex spectrum. This band is assigned to a C–H stretch vibration, but one that involves a different kind of motion not found in the four-coordinate species: the motion of two C–H's on acetylenes coordinated to the metal vibrating into the π -cloud of the external acetylene molecule. This is essentially a weak hydrogen-bonding interaction that binds the outer molecule, and like hydrogen-bonded OH stretches, this causes the hydrogen stretch involved to be significantly red-shifted. Because the vibration penetrates into the π -cloud of the outer acetylene, the dipole derivative is large, and this mode has a high predicted IR intensity. We are therefore quite sensitive to the possible presence of this 3+1 isomer. However, there is only broad, weak structure in the spectrum near 3179 cm^{-1} , indicating at most a very small amount of this 3+1 isomer. DFT is well known to have trouble with weak van der Waals interactions,^{16,60} and it apparently overestimates the stability of the 3+1 isomer in the present system.

Trends through the Complexes. Our infrared spectra and DFT calculations make it possible to observe trends that run through these $\text{Ni}^+(\text{C}_2\text{H}_2)_n$ complexes. The first interesting pattern is the binding energies of the acetylene ligands to the Ni^+ . For example, the sequential bond dissociation energies (BDE) for the detachment of a single C_2H_2 ligand can be estimated from the B3LYP results. As can be seen in Table 1, the bond dissociation energies for the process $\text{Ni}^+(\text{C}_2\text{H}_2)_n - \text{C}_2\text{H}_2 \rightarrow \text{Ni}^+(\text{C}_2\text{H}_2)_{n-1}$ are 47.0, 38.4, 16.1, and 4.9 kcal/mol for the $n = 1-4$ complexes, respectively. There is a significant drop in

BDE when going from $n = 2$ to $n = 3$, and the fourth acetylene is much more weakly bound again. This is consistent with dissociation energies measured for similar complexes. Bowers and co-workers measured the BDEs of $\text{Ag}^+(\text{C}_2\text{H}_2)_n$ complexes with equilibrium mass spectrometry and compared their results to theory.¹⁷ They determined that this system was also four-coordinate and observed a significant drop in the binding energy after $n = 2$. In this case, elimination of acetylene from the $\text{Ni}^+(\text{C}_2\text{H}_2)_3$ complex requires $\sim 5600\text{ cm}^{-1}$ of energy, which is still greater than the energy of a single photon near 3300 cm^{-1} . However, DFT predicts that only 1700 cm^{-1} is needed to dissociate the $n = 4$ complex, and this should photodissociate via a single-photon process in the C–H stretch region. These predictions are completely consistent with our observations. Photofragmentation was inefficient for $\text{Ni}^+(\text{C}_2\text{H}_2)_3$, whereas the $n = 4$ complex dissociated easily.

The DFT calculations run contrary to the experiment regarding the coordination numbers for acetylene around Ni^+ . The 3+1 and four-coordinate isomers at the $n = 4$ complex are predicted to have virtually the same energy, and in fact the 3+1 isomer is predicted to be slightly more stable. However, the experimental breakdown pattern in Figure 1 clearly shows that the coordination is 4. Likewise, the spectrum in Figure 6 finds little evidence for the 3+1 isomer. Apparently, DFT overestimates the stability of the acetylene in an external hydrogen-bonding configuration. Related to this, we have found that structures in which acetylene is allowed to cyclize, forming either π -bonded cyclobutadiene or benzene, are calculated to be even more stable than the four-coordinate or 3+1 structures presented here.⁶² We will elaborate on such reacted structures at the $n = 4$ and larger cluster sizes in a future paper.⁶² However, the excellent agreement between the experiment and theory shows that these reacted structures are not needed to explain our spectra for the $n = 4$ (or smaller) complexes studied here. On the other hand, it should be noted that in the present experiment we detect only those $n = 4$ complexes with a weakly bound acetylene. Our calculations on reacted $n = 4$ structures find that these do not have any acetylene ligands that could be one-photon dissociated in the C–H stretch region. It may then be that we are blind in the experiment to such reacted structures, because they would not dissociate efficiently without tagging. However, as noted above, we are not able to obtain efficient tagging for complexes with more than three ligands. An investigation of various possible reaction products in the $n = 4-8$ complexes, and the comparison of their spectra to similar IRPD measurements, is the topic of our future paper.⁶²

A second pattern in these data is the shift of the IR bands for different cluster sizes. Figure 7 shows the IRPD spectra of $\text{Ni}^+(\text{C}_2\text{H}_2)\text{Ne}$, $\text{Ni}^+(\text{C}_2\text{H}_2)_{2,3}\text{Ar}$, and $\text{Ni}^+(\text{C}_2\text{H}_2)_4$ to illustrate how the C–H stretches evolve as more acetylenes are bound to the cation. The spectra and theory for the $n = 1-4$ complexes show that the binding distorts the geometry of the acetylene moieties by weakening the $\text{C}\equiv\text{C}$ bond and pushing the hydrogens away from linear. Therefore, the symmetric stretches all become IR active, and all the C–H resonances occur at lower frequency than the pure acetylene vibrations. As more ligands are added, the individual Ni^+ –acetylene π -bonds weaken, as the binding capacity of Ni^+ is distributed over more ligands, resulting in

(62) Pillai, E. D.; Walters, R. S.; Schleyer, P. v. R.; Duncan, M. A., to be submitted.

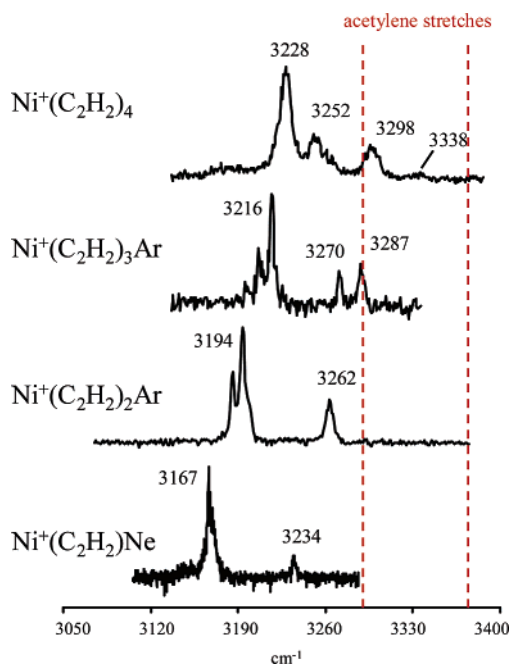


Figure 7. IRPD spectra of the $n = 1-4$ complexes from 3100 to 3400 cm^{-1} . As subsequent acetylenes are added to the nickel cation, the C–H resonances blue-shift back toward the free acetylene modes.

less perturbed C–H modes. Therefore, the bands shift back toward the free acetylene frequencies as cluster size increases, as shown in Figure 7. This trend persists, even though different isomeric species may be present at each cluster size. The shifts from rare gas atoms, regardless of the isomeric binding sites, are always smaller than the shifts induced by acetylene. The main consideration in the position of the C–H stretch vibrations is the number of π -bonded acetylenes present.

A final pattern running through these data is the occurrence of low-symmetry structures for the binding of multiple acetylene ligands around the nickel cation. We do not find any evidence for two ligands in a D_{2h} structure, for three ligands in a D_{3h} structure, or for four ligands in a square-planar (D_{4h}) structure. The four-coordinate complex has a structure that is close to, but distorted from, tetrahedral. The lower symmetry structures found are in contrast to our studies on multiple ligand binding around other transition metal ions and also for the clustering of other ligands around Ni^+ . Our previous studies found that high-symmetry structures are produced for the clustering of CO_2 around Fe^+ , V^+ , and Ni^+ ,³⁶ for N_2 clustering around V^+ ,⁴⁰ and for the clustering of H_2O around Ni^+ .^{39c} CO_2 and N_2 bind through more electrostatic interactions and are more compact because they bind in an end-on configuration. As noted earlier, Jahn–Teller distortion is likely for Ni^+ , but this should be more important for ligands with a greater covalent fraction in their binding. Acetylene is perhaps the worst case for symmetric structures because it has a high fraction of covalent bonding. This, together with the electronic structure of Ni^+ , increases the importance of Jahn–Teller distortions, which are seen even in the small clusters where steric effects are not important. Because acetylene binds side-on, it is sterically difficult to arrange multiple ligands around the metal, and this factor probably also influences the structures of the $n = 3$ and 4 complexes. It will be interesting to study multiple-acetylene complexes with other transition metals to see if higher symmetry structures occur.

Closely related to the low-symmetry geometries is the multiplet structure that arises in the C–H region for several of these clusters. DFT predicts low-lying isomeric structures associated with different argon attachment sites, and it predicts low-lying excited states for all of these complexes. These effects provide plausible mechanisms for the multiplet structure seen. However, in the case of the $n = 3$ complex, we have the puzzling behavior where the predicted spectrum is quite different with the two basis sets studied. Likewise, if we believe the predictions of DFT, it is not clear why we do not have evidence of isomers and excited states for *all* of the complexes. It is well known that DFT has difficulties in properly describing weak van der Waals forces and in predicting the relative energies of different electronic states.^{16,60} Therefore, the importance of these issues may be overestimated in many of these complexes. In the $n = 4$ complex, this is definitely the case, as the 3+1 isomer is predicted to have essentially the same energy as the four-coordinate species, but there is virtually no evidence for this in the spectrum. More advanced theoretical treatments of these complexes will be needed to resolve some of these questions. However, studies employing methods other than DFT remain quite challenging for systems as complex and chemically interesting as these.

Conclusions

Nickel cation–acetylene complexes containing up to four acetylene ligands are studied with infrared photodissociation spectroscopy and density functional theory. The attachment of rare gas atoms is necessary to measure photodissociation spectroscopy for most of these systems, but this produces only minor perturbations on the structures and the infrared spectra. Photodissociation patterns indicate that the Ni^+ ion binds four acetylene ligands in its coordination sphere. Both experiment and theory agree that π -complexes are formed for all clusters studied up to $n = 3$. At the $n = 4$ cluster, a 3+1 isomer is predicted to lie at low energy, but the experiment finds little or no evidence for it. The spectrum of $n = 4$ fits nicely with predictions for a four-coordinate π -complex. In each of the complexes studied, the metal ion–ligand interaction distorts the acetylene geometry, weakening the $\text{C}\equiv\text{C}$ bond and pushing the hydrogens off the $\text{C}\equiv\text{C}$ axis. This distortion activates the symmetric C–H stretch in the infrared and shifts both C–H resonances to lower frequency. Low-lying electronic states are predicted for all of these complexes, but it is difficult to find direct evidence for these states in the spectra. In the $\text{Ni}^+(\text{C}_2\text{H}_2)\text{-Ar}_2$ complex, four bands observed in the spectrum could arise from either two structural isomers or two electronic states that are nearly isoenergetic. Larger complexes could also have contributions to their spectra either from excited states or from other isomeric structures. It is impossible to distinguish these effects in the spectra of the $n = 2$ and 3 complexes. Theory suggests that isomers arise from different arrangements of the acetylene ligands ($n = 2$) and from different rare gas attachment sites ($n = 2$ and 3) in these complexes, but unexpected behavior is found in the treatment of the $n = 3$ complex with different basis sets. Asymmetric acetylene attachment is predicted by DFT for all the multiligand complexes, apparently arising from Jahn–Teller distortion caused by the electronic configuration of Ni^+ . Symmetric ligand attachment would give rise to “simple” two-peak spectra in the C–H region, but this is not detected for any multiligand complex. Even though isomers or excited

electronic states are needed to explain the fine details of the multiplet structure seen, the most important consideration determining the position of the C–H bands is the number of acetylene ligands in the complex.

This is perhaps the most extensive investigation yet combining IR spectroscopy and theory to examine the progressive binding of multiple ligands around a transition metal in the isolated gas-phase environment. It is clear that describing the electronic structure of such multiligand complexes is quite challenging. DFT is necessary to be able to treat multiligand complexes for a metal like nickel, but its energetic predictions for different isomeric species are problematic. The experimental measurement of these spectra is also complex, as it requires the presence of rare gas tag atoms. Likewise, it is clear that the interpretation of these spectra in the C–H region and how they can be used to distinguish different isomers is not straightfor-

ward. At present, these experiments are limited to the C–H stretching region by the available infrared lasers. However, as new IR sources become available, it will be important to extend these studies further toward longer wavelengths where other IR modes may be detected.

Acknowledgment. We appreciate the support of this work by the U.S. Department of Energy through grant DE-FG02-96ER14658.

Supporting Information Available: Full citation for ref 46; full results of our density functional theory calculations on the various $\text{Ni}^+(\text{C}_2\text{H}_2)_n(\text{RG})_m$ complexes, including structures, energetics, and vibrational frequencies for the different isomeric structures at each cluster size. This material is available free of charge via the Internet at <http://pubs.acs.org>.

JA054800R